Letter

Ecological causes of uneven speciation and species richness in mammals

Short title: Ecology of speciation in mammals

Nathan S. Upham[1*], Jacob A. Esselstyn[2], and Walter Jetz[3]

Author affiliations:

[1]Department of Ecology & Evolutionary Biology, Yale University, New Haven, CT 06511 USA, nathan.upham@yale.edu. [2]Department of Biological Sciences and Museum of Natural Science, Louisiana State University, Baton Rouge, LA 70803 USA, esselstyn@lsu.edu. [3]Department of Ecology & Evolutionary Biology, Yale University, New Haven, CT 06511 USA, walter.jetz@yale.edu.

*Corresponding: 165 Prospect St., OML 122, New Haven, CT 06511 nathan.upham@yale.edu.

Statement of authorship: NSU and WJ conceived the study; NSU and JAE collected and curated the data; NSU performed all analyses and wrote the first draft of the manuscript, with contributions to revisions from all co-authors.

Data and material availability: All data and code is available in the manuscript and after publication on Dryad (also to be available at github.com/n8upham/).

Keywords: Phylogenetics, macroevolution, trait-associated diversification, dispersal, latitude, diel activity; **Length:** abstract 172 words; main text 4,710 words; 110 references; 5 figures.

ABSTRACT

Biodiversity is distributed unevenly from the poles to the equator, and among branches of the tree of life, yet how those enigmatic patterns are related is unclear. We investigated global speciation-rate variation across crown Mammalia using a novel time-scaled phylogeny (*N*=5,911 species, ~70% with DNA), finding that trait- and latitude-associated speciation has caused uneven species richness among groups. We identify 24 branch-specific shifts in net diversification rates linked to ecological traits. Using time-slices to define clades, we show that speciation rates are a stronger predictor of clade richness than age. Speciation is slower in tropical than extra-tropical lineages, but only at the level of clades not species tips, consistent with fossil evidence that the latitudinal diversity gradient may be a relatively young phenomenon in mammals. In contrast, species tip rates are fastest in mammals that are low dispersal or diurnal, consistent with models of ephemeral speciation and ecological opportunity, respectively. These findings juxtapose nested levels of diversification, suggesting a central role of species turnover gradients in generating uneven patterns of modern biodiversity.

INTRODUCTION

Biological diversity is concentrated at the equator more than the poles, and in some evolutionary lineages more than others. Yet whether these organic phenomena are causally connected is an open question. The latitudinal diversity gradient is generally attributed to tropical biomes being stable, productive, and old (1–5), but there is less consensus regarding why species richness is distributed unevenly across the tree of life. Phylogenetic tree shape was first characterized taxonomically (6) and later formalized under the concept of tree imbalance or unevenness (7). To arise, more speciose clades must have been derived from faster rates of net diversification (speciation – extinction), older ages (earlier divergences), or both. However, the relative contribution of clade rates and ages to species richness is widely disputed (e.g., (8–11)). Similarly controversial are the causes of diversification-rate variation in real phylogenies, whether due to stochasticity, determinism via ecological factors or time, or artifacts from how we reconstruct evolutionary history (12–23). Latitude might determine the rates at which new species originate and persist or go extinct (2, 3, 24–26), but so too might species' intrinsic traits (27), some of which are correlated with latitude (e.g., (28)). For mammals and other tetrapods, the Cretaceous-Paleogene (K-Pg) bolide impact is linked to the selective extinction of major lineages (29, 30), adding the wrinkle of historical contingency to how surviving lineages diversified in response (31–33). Thus, understanding the processes underpinning uneven species richness requires connecting levels of indirect (e.g., eco-geographic) and direct (e.g., rates, ages) causes to tease apart their joint influences upon different radiations.

The last ~180-million-years of crown mammalian evolution has resulted in ~6000 living species (34, 35), which collectively inhabit nearly all terrestrial biomes plus the open oceans, and thousands of preserved ancestors described as fossil taxa (36–38). Within this context, similarly

aged clades in the mammal tree range from mega-diverse rodents (~2500 living species) and bats (~1300 species) to species-poor groups like treeshrews (20 species) and pangolins (8 species; all four share stem ages of ~60-70 million years ago [Ma] (35, 39)). The early availability of a species-level 'supertree' phylogeny of mammals (now cited over 1,800 times; (40)) encouraged initial studies of macroevolutionary-rate covariates (e.g., (18, 22, 41, 42)). However, because that pioneering supertree was assembled from hundreds of overlapping source trees, over 50% of its nodes were initially unresolved and then simulated to obtain a bifurcating time-scaled phylogeny (40, 43). Timings of diversification from this supertree, along with two other mammal supertrees (11, 44), were consequently shown to have inflated precision relative to the large gaps in available fossil age and DNA sequence data (35).

Here, we draw upon a new time-calibrated phylogeny for global Mammalia built from a contiguous DNA supermatrix (31 genes by 4,098 species; completed to 5,911 modern species) and consisting of credible sets of 10,000 trees (35). We used these phylogenies, which jointly model uncertainty in topology and node ages, to better understand the temporal dynamics of mammalian diversification relative to the potentially causal effects of historical, organismal, and environmental factors. Our objectives were three-fold. First, we tested for tree-wide and branch-specific rate variation in relation to the Cretaceous-Paleogene (K-Pg) mass extinction event to explore whether predicted shifts in placental diversification rates (45) are recoverable across extant clades. Second, we used neutrally defined (time-slice based) clades to explore the relative roles of clade ages and speciation rates in explaining current-day species richness. Finally, we linked observed variation in speciation rates to its putative ecological causes, testing whether factors predicted to cause newly formed species to persist or go extinct are, in turn, causing the observed patterns of uneven species richness. Investigating deep-time rate shifts (e.g., relative to

the K-Pg or other factors) alongside the drivers of modern clade richness is intended to test for time-specific differences in the drivers of mammalian rate variation.

Among clades, we focus on three potential ecological causes of richness differences: species vagility, latitude, and diurnality. First, we tested whether low-vagility species have faster speciation than more dispersive species given their greater likelihood of forming peripheral isolates (46, 47). For this test, we developed an allopatric index of organismal vagility for all mammals (i.e., maximum natal dispersal distance; (48)). Vagility effects have never been assessed across all mammals, although evidence in birds using the hand-wing index supports an inverse vagility-to-speciation rate relationship (e.g., (49, 50)). Second, if unstable environments increase ephemeral speciation via greater species turnover (extinction / speciation (51)), then we expect the recent species-specific (i.e., 'tip') speciation rates of surviving lineages to be higher in temperate latitudes with greater climatic instability (25, 52). To our knowledge, the effects of latitude upon mammal tip rates have yet to be assessed, but clade-level comparisons have either been negative (53) or supported greater temperate than tropical turnover in some clades (24, 42, 54). Lastly, we tested whether diurnality (daytime activity) has increased speciation rates relative to nocturnal clades, following recent evidence that all mammals were nocturnal until daytime niches evolved ~35 Ma (33, 55). A positive influence of diurnality on speciation rates has been found across major tetrapod lineages (56), and in primates specifically (57, 58), but has yet to be investigated at the species-level in all mammals (but see ancestral state reconstructions (55)). We are thus using species-level trait proxies to investigate scenarios of geographic, ephemeral, and adaptive modes of species diversification in mammals, respectively, and across the entire mammal tree of life to avoid ascertainment bias from selecting smaller clades (59).

Overall, our approach ties together among-clade variation in rates, ages, richness, and traits in a multivariate causal framework (phylogenetic path analysis (60)). By jointly assessing the causal contributions of ecological factors to the inferred tempo of mammalian lineage diversification, we shed new light on their relative importance to generating uneven species richness patterns. We find that vagility and diurnality are greater causes of recent speciation-rate variation than latitude, which effects rates deeper in the tree. Rate variation, in turn, contributes more to uneven species richness than differences in clade age.

RESULTS AND DISCUSSION

Tree-wide lineage diversification relative to the K-Pg event.

The Mammalia tree shows substantial unevenness in species richness across major named clades (Fig 1a). We first evaluated evidence for whether early placentals diverged before, after, or during the K-Pg event, known as the short fuse, long fuse, and explosive models, respectively (45, 61). The first four placental divergences unambiguously preceded the K-Pg (Fig. 2a; filled circles), followed by the next 21 divergences with CIs that overlap it (Fig. 2a–b). Therefore, we detect a Cretaceous "fuse" of ~25-Ma between the radiation of crown Placentalia and nine of 18 crown orders (Fig. 2b), in line with some estimates (39, 62), but longer than others (e.g., (40)).

Modeling branch-specific rates across the tree shows a qualitative pulse in both speciation and extinction near the K-Pg (Fig. 2c) that matches concurrent fossil evidence for increases in origination and extinction (Fig. 2d; synthesized from the Paleobiology Database (37)). However, we find mixed results in formal tests of tree-wide shifts in the 5-Ma following the K-Pg, with TreePar (41) showing a clear signal of increased net diversification rates that is absent in CoMET analyses (63) ((Fig. S5-S6); the latter model allows for time-varying

130 diversification rates while the former does not). Based on the patterns reported in fossil
131 eutherians (45, 64), a pulse of lineage turnover following the K-Pg is expected due to selective
132 extinction and recovery of surviving mammal lineages (29, 31). Thus, this fossil-calibrated
133 molecular phylogeny of mammals (35) is capable of recovering dynamics evident from the fossil
134 record alone, albeit as dependent upon assumptions of different tree-wide birth-death models.
135
136 **Branch-specific rate shifts relative to time and traits.**
137 We recover shifts in net diversification rates associated with 24 consistent nodes in the
138 mammal tree (Fig. 1a, 2c, e; shifts are present in ≥ 50% of maximum shift credibility trees using
139 BAMM (65), see *Supplementary Materials* Fig. S7, Table S1). The earliest rate shift occurs in
140 either crown Placentalia (mean of 1.1x higher over separate BAMM runs, as compared to the
141 median background rate of 0.138 species/lineage/Ma) or Boreoeutheria (1.6x, node C in Fig. 1a).
142 These shifts involve 18 different lineages, 15 of which are consistent increases. The only
143 consistent rate decrease was in the strepsirrhine primates (lemurs, lorises, and galagos; node O).
144 Two other shifts are alternately up or down, depending on the tree sampled (nodes H, P; Fig. 1a).
145 This result compares to 27 rate-shifted clades detected on the original mammal supertree using
146 an earlier method (15 increasing and 12 decreasing (18)—but note caveats about the
147 identifiability of downshifts (66)). Overall, rate increases nearer the present are higher, with a
148 2.2x mean in the Miocene versus 1.3x in each the Oligocene and Eocene (Fig. 2c; df=2, F=7.772,
149 P=0.003). This result is consistent with the expectation for extinctions deeper in the tree to have
150 reduced our ability to quantify more ancient shifts (65, 67), as well as fossil and molecular
151 evidence that younger clades tend to have faster rates of diversification (20).

152 At first glance, species in rate-shifted clades have dissimilar traits of vagility, diurnality,
153 and latitudinal extent (Fig. 1a-b). However, several consistent patterns emerge. On a visual basis,
154 related clades of rodents show a conspicuous latitudinal pattern of alternating south-north-south
155 endemism that may relate to biogeographic incumbency effects previously reported (e.g., (68)).
156 Similarly, the rate shifts present in Cetacea and Carnivora (nodes F and D; Fig. 1a) are associated
157 with high vagility and latitudinal extents, while simian primates (node N) are nearly exclusively
158 tropical and diurnal (Fig. 1b). Strikingly, the two largest rate increases (4.0x and 3.2x) occurred
159 in lineages with disparate life modes but similar propensities for geographic isolation: the
160 fossorial tuco-tucos of South America (*Ctenomys*, node Q), and the Indo-Pacific flying foxes
161 (*Pteropus*, node J; Fig. 1a). Thus, small burrowers and large flyers both show similar signatures
162 of recent and rapid speciation under conditions of insularity, although in subterranean and
163 oceanic realms, respectively. Ecologically selective processes appear to be involved in fostering
164 major mammalian radiations, but are these trait associations idiosyncratic or deterministic?
165 We next investigated trait-dependent speciation on a tree-wide basis, aiming to look for
166 common ecological causes of rate variation. These tests uncovered that high vagility is
167 marginally associated with novel rate regimes (STRAPP (69) one-tailed test, $P = 0.08$), which is
168 contrary to the inverse vagility-to-speciation relationship we expected (46, 47). However, these
169 tests are complicated by the fact that many high-vagility lineages are also diurnal, and diurnality
170 is clearly associated with shifts to higher speciation-rate regimes ($P = 0.027$; Fig. S8). For
171 example, we find diurnality-associated rate shifts in clades of primates, carnivorans, cows, and
172 whales (shifts N, D-F, and Q; Fig. 1a) that also contain a majority of species with >1 km natal
173 dispersal distance (Fig. 1b). Therefore, these findings highlight the need to jointly consider (i.e.,

174 in the same model) the relative contributions of vagility, latitude, and diurnality to understand
175 their effects upon rate heterogeneity in mammalian clades.
176
177 **Named clade rate variation.**
178 Beyond searching for rate-shifted clades, we also test the five most speciose placental
179 orders for signatures of diversification-rate variation (Fig. 2e-f). Comparing the fit of models of
180 rate-variable processes through time (RV, exponential or linear; (70)) versus rate-constant ones
181 (RC, single rates of birth or death), we find greater fits to RV models in five of the 12 named
182 subclades examined (Fig. 2f; Table S2). The mouse-related clade of rodents (clade 20 in Figs. 1,
183 2f) has a branching pattern best fit by RV processes in all 100 trees examined, as expected from
184 the seven branch-specific rate shifts already uncovered in that clade (nodes R-X in Figs. 1, 2).
185 Shrews, catarrhine primates, and the cow- and whale-related clades of artiodactyls join mice in
186 showing greater RV fits than expected from RC simulation (clades 6, 15, 10, and 11; Fig. 2f).
187 Overall, these named clade results are consistent with previous evidence (e.g., among mammal
188 families (21)) that lineage diversification rates have been non-constant through time.
189 In theory, considerably more fossil evidence might be required for the birth-death models
190 evaluated so far to be identifiable (71). This word of caution is particularly relevant for groups
191 like horses and pigs (Perissodactyla (72)), in which we know that periods of diversity decline
192 have been substantial (see (73) for general comparison of BAMM and RPANDA model
193 performance). Nevertheless, clade-specific fossil and molecular evidence supports our assertion
194 that ancestral whales and dolphins entered a novel macroevolutionary regime, including selection
195 toward larger body sizes (65, 69, 70, 74). Bats, on the other hand, display an inconsistent fit to
196 RV models of diversification (clades 12-13, Fig. 2f), and an inconsistent number of rate shifts

197 between our study (six, nodes G-L, Fig. 1a) and a previous one (two, nodes H and J; (75)). We
198 suggest that high levels of topological uncertainty, which is arguably greater in bats than other
199 orders (76), is contributing to the equivocal modeling of RC, RV, and branch-specific shift
200 processes across credible tree sets for bats (Table S2).

201 As an alternative, non-model-based test of within-clade rate variation, we use clade-wide
202 distributions of tip-level speciation rates as assessed using the tip DR metric (77) (Fig. 2f). Tip
203 rates carry the benefit of estimating diversification dynamics at the instantaneous present, and
204 thereby overcome the aforementioned concerns regarding the impact of past extinctions on
205 model identifiability (71, 73, 78, 79). Broadly, we recognize substantial heterogeneity in tip
206 speciation rates across the mammal tree, sometimes with a few high-tip-rate species nested
207 together with lower-rate species (Fig. 1a), resulting in long right-side tails in the tip-rate
208 distributions (positive skew, e.g., bat and rodent clades 12 and 18; Fig. 1a, 2f). We propose that
209 tip rate skew measures aspects of within-clade speciation-rate variation that is otherwise
210 uncaptured by fitting *a priori* models of the diversification process (Table S3), and thus offers a
211 distinct predictor of among-clade variation in species richness.

212

213 **Time-slice clade richness relative to ages and rates.**

214 The relative importance of clade ages (time) versus rates of speciation and extinction
215 (whether stochastic or ecologically deterministic) as an explanation of extant diversity levels is
216 widely debated (8–12, 16, 21, 80). Original claims that uneven trees are random outcomes of
217 constant-rate diversification (e.g., (81)) have been refuted (10, 13, 17). However, past efforts to
218 separate these hypotheses have focused on named clades (e.g., (10, 21)), which are biased by
219 subjective delineation and often vast age differences (mammal families range 3.8–59.0 Ma in

mean crown ages; (35)). To avoid problems associated with subjective clade definitions, we sliced phylogenies at five-million-year intervals and took the tipward clades as objective units for analysis (Fig. 3). Time-sliced clades thus account for the 'pull of the present' in modern trees (67) by analyzing successive levels of rootward covariance among clade-level summaries of crown age, species richness, tip rate harmonic mean and skew, and the arithmetic (or geometric) mean of species ecological traits. If time-constant rates predominate (11, 12, 16), crown ages will explain the most among-clade variation in species richness. In contrast, if rate variation is strong, as we already recognized for some nodes and named clades (Fig. 2) and expect from varying ecological regimes (18, 22, 23), diversification rates will have the greater explanatory power.

We find that the clade harmonic mean of tip speciation rates explains most of the variation in species richness across time-sliced clades (Fig. 4, multivariate PGLS). Clade age and richness are positively correlated (Fig. 4a)—yet clade tip rate mean has stronger effects on richness than expected from simulated birth-death trees containing only stochastic rate variation (Fig. 4b). Clade tip rate skew is also significant, especially so at deeper time slices (Fig. 4c), confirming that single speed-ups in diversification within a clade (e.g., due to a rate shift in one lineage) can drive much of its overall species richness today. These analyses are robust to the influence of species that are missing DNA sequences and imputed (see Fig. S10, also for univariate and taxon-based results). Our findings thus support arguments that 'ecology' (broadly defined to include any non-temporal factor that alters macroevolutionary-rate processes, including sexual selection and geographic factors) is a greater cause of species richness variation than time (21–23). However, variation in both rate and age clearly contribute to observed richness (adjusted-R^2: 0.88 full model versus 0.74 with tip rate mean only and 0.26 with crown age only, means of 100-tree PGLS among 35-Ma clades). Jointly analyzing richness

243 determinants in time-sliced clades offers an objective way to assess age and rate effects that, in
244 turn, raises questions about which ecological factors are driving that rate variation.
245
246 **Linking uneven rate variation to ecological factors.**
247 We performed phylogenetic path analysis (60) to assess the hypothesized effects of
248 species vagility (46, 47), latitude (24, 25), and diurnality (33) upon the joint, yet unequal,
249 contributions of rates and ages to extant species richness variation (Fig. 5, *Methods*, Fig. S4).
250 Here, the time-sliced clades allow us to distinguish trait-rate dynamics that are localized near the
251 species level (if traits drive species turnover (51), or if they evolved very recently) from those
252 that occur among clades deeper in the tree (if traits evolved anciently and the lineages persisted).
253 Our assembly of species-level traits across Mammalia (Fig. 1b) enables us to directly pass
254 information to clade-level averages, thereby summarizing the ecological 'essence' of that clade
255 for a given trait. However, we note that other statistical moments (e.g., trait variance or skew)
256 may prove useful for future study.
257 At the species level, we find that low-vagility mammals have higher tip speciation rates,
258 especially in herbivores and carnivores (Fig. 5a; ecological trait ~ rate PGLS (82)). Effects of
259 vagility on clade tip rate mean in 10-Ma clades are weakened at deeper time slices, where they
260 are instead recorded on tip rate skew (Fig. 5b). We interpret these short-lived effects of vagility
261 on speciation rates as consistent with expectations that incipient species are produced at a high
262 rate, but are ephemeral (51), subject to high species turnover. Under this scenario, speciation
263 rates are roughly constant, but low-vagility lineages have gone extinct at a faster rate than high-
264 vagility forms, presumably due to the stochastic effects of small geographic range size in nascent
265 species (47, 83). In summary, we hypothesize that turnover-driven speciation—i.e., speciation

266 rates that are high because extinction rates are high, and a lineage is still observed—is causing
267 the inverse effects of vagility upon tip speciation rates we observe in the mammal tree.
268 Our interpretation argues for an approximately 10-million-year 'threshold' whereby low-
269 vagility lineages must lower their extinction risk (e.g., find an adaptive zone or evolve greater
270 vagility; (84, 85)) or else vanish. Alternatively, the influence of vagility on mammal
271 diversification might be non-linear as hypothesized in birds (e.g., humped (46) or sigmoidal
272 (50)), in which case our results among shallow clades and tip species may only be capturing one
273 side of the vagility-to-rate relationship. We concede that our allometric vagility index is a rough
274 proxy for dispersal ability, particularly given the potential for island effects in the nearly 20% of
275 living mammals that are endemic to islands (86). Similarly, the vagility index does not explicitly
276 account for the flying abilities of bats, which differ substantially by wing morphology (87).
277 Nevertheless, the described patterns are robust to multiple sensitivity tests (including the
278 exclusion of bats and island endemics; (Fig. S13-S14)), and thus are deemed to convey the
279 macroevolutionary outcome of historical gene flow or isolation among populations of mammals.
280 To test the causal role of environmental stability in the generation of mammalian tree
281 shape (3, 25, 52), we next evaluated how a climatic proxy—latitudinal centroid distance from the
282 equator—influences speciation rates. Contrary to the expectations of climatic instability driving
283 recent, high rates of speciation at temperate latitudes (24, 25, 52), we find no effect of absolute
284 latitude on tip-level speciation (Fig. 5a). Instead, strong positive associations with latitude only
285 arise among clades at deeper time slices, and without any corresponding effects on clade tip rate
286 skew (Fig. 5b). These results compare to similarly absent latitude-to-tip rate effects in the
287 species-level phylogeny of birds ((77, 88); but see suboscines (89)). For both birds and
288 mammals, New World sister species show higher turnover rates at temperate than tropical

289 latitudes (24, 52); however, reliance on the mitochondrial DNA clock renders these results less
290 conclusive for mammals than birds given their more pronounced life-history effects (90). Other
291 mammal studies have yielded inconsistent findings with a variety of methods, including: (i)
292 higher subspecies counts in harsher temperate environments ((54); but note the opposite pattern
293 in birds (91)); (ii) no latitude-to-rate effects at the genus level (53), using genus ages from the
294 Bininda-Emonds et al. (40) supertree of mammals; and (iii) greater rates of temperate extinction
295 and tropical speciation on a Mammalia-wide basis (42), using a modified version of the same
296 supertree. Thus, our finding that temperate clades of mammals have higher tip rates than tropical
297 clades (harmonic mean of species values at 10-, 30-, and 50-Ma time-sliced clades) sheds new
298 light on what, to date, has been a murky understanding of how macroevolutionary rates have
299 influenced the latitudinal diversity gradient.

300 We hypothesize that high rates of temperate extinction during the Plio-Pleistocene, a
301 period of harsh environmental changes starting ~5 Ma (92), may have erased the modern portion
302 of the latitudinal effect that otherwise would be recorded in species' present-day tip rates. Under
303 this scenario, finding clade-level signatures of faster temperate speciation (as we did) is still
304 expected as long as temperate lineages were not fully extirpated during these climatic
305 oscillations, perhaps as persisting in glacial refugia (93). Key to understanding this result is that
306 the latitude-to-rate signature among, e.g., 30-Ma clades reflects processes occurring *more*
307 *recently* than 30 Ma, since we are examining clade-level summaries of branching rates leading to
308 each species' instantaneous present. Thus, we are proposing that intensified Pliocene rates of
309 temperate extinction initiated two canonical patterns, at least in mammals if not other taxa: (i) the
310 inverse latitudinal gradient of clade-level speciation rates, as viewed retrospectively on an extant
311 phylogeny; and as a result, (ii) the latitudinal diversity gradient. This hypothesis is supported by

312 the North American fossil record (the most complete paleogeographic sampling of mammals), in
313 which richness and latitude are not strongly correlated until ~4 Ma (94), as well as evidence from
314 fossil bivalves that Pliocene extinctions strengthened the latitudinal diversity gradient (95).
315 Overall, we contend that the traditionally invoked tropical 'cradle' (higher speciation) and
316 'museum' (lower extinction (3)) should instead re-focus upon the *turnover ratio* of those
317 processes. Testing whether species lineages have been 'cycled' faster (i.e., shorter durations)
318 outside than inside the tropics is a prediction in need of greater paleo-to-neontological synthesis.
319 Lastly, we queried the effect of diurnal diel activity, a core behavioral trait thought of as a
320 temporal niche innovation (33). We find that apparently independent origins of diurnality since
321 the late Eocene (~35 Ma (33, 55)) are associated with faster speciation, both at the present (Fig.
322 5a) and among time-sliced clades at 10 Ma (Fig. 5b). These findings complement the signature
323 of greater diurnal activity on rate-shifted clades (Fig. S8), as well as place previous findings of
324 rapid diversification in diurnal lineages of primates (57, 58, 96) and whales (70) in a broader
325 context. We suggest that inverse effects of diurnality on tip rate skew at deeper time slices (Fig.
326 5b) are misleading given the evolution of daytime activity ~35 Ma, well after a 'nocturnal
327 bottleneck' among K-Pg-surviving mammals (33, 55). This bottleneck has been described at
328 broader phylogenetic scales across major extant lineages of tetrapods (family-level sampling for
329 mammals (56)), although fossil evidence suggests that daytime activity also evolved in the
330 extinct sister lineages to mammals (non-mammalian synapsids (97)). The coordinated eco-
331 physiological changes required to evolve diurnality (e.g., eye pigments and corneal size (33))
332 have presumably carried with them fitness benefits from access to novel resources in the daytime
333 niche. Thus, diurnality may rightly be viewed as an adaptative innovation in mammals, and one
334 that appears to have induced macroevolutionary rate changes.

335 To explain faster speciation in diurnal clades and species, we posit that greater daytime
336 activity is an example of a trait that has decreased extinction rates via competitive release (i.e.,
337 an 'ecological opportunity'; (84, 98)). In this scenario, evolving diurnality has led to differential
338 lineage persistence (i.e., low rates of species turnover = low extinction / high or moderate
339 speciation) relative to nocturnality because novel niche resources have presumably improved
340 organismal fitness (33, 84). This hypothesis implies that persistence-driven speciation—i.e.,
341 speciation rates that appear high because extinction rates are reduced—underlies the diurnal rate
342 signature, in contrast to the turnover-driven speciation we suggest is associated with low-vagility
343 and high-latitude lineages. Alternatively, the more classical narrative of 'key innovation'
344 spurring diversification (84) would suggest that diurnal lineages have increased speciation rates
345 (with no change in extinction) due to specializing on resources within the relatively 'open'
346 diurnal ecospace. While we cannot rule out this speciation-only hypothesis, we find it less
347 probable because the acquisition of diurnal behavior has likely evolved and persisted at least ten
348 times in crown mammals (55). From diurnal primates and squirrels to elephant shrews, there
349 seems to be no characteristic secondary axis of resource specialization that is common to these
350 groups (e.g., diet or locomotor diversity); rather, allopatric speciation—and persistence of those
351 lineages—is more likely the secondary driver of diurnal diversity (e.g., (99)) following the initial
352 adaptation. Overall, we suggest that faster diurnal than nocturnal speciation in mammals is a
353 signature of greater persistence (lower turnover) of lineages due to more ecological opportunity.
354

355 **CONCLUSION**

356 By taking an uncommonly broad view on the evolutionary history of Mammalia, from
357 tree-wide to branch-specific to tip-level processes, the present study uncovers commonalities in

358 the ecological causes of uneven species diversification over geography as well as phylogeny.
359 These general processes might have remained hidden had this study been motivated by
360 publishable units and not global synthesis. Using an innovative time-slice approach to defining
361 clades, we demonstrate that clade rates explain more of the variation in mammal species richness
362 than do clade ages. Connecting those clades rates to both intrinsic (vagility, activity pattern) and
363 extrinsic (latitude) characteristics of the component species, we then detect consistent ecological
364 signatures at nested levels of the mammal phylogeny.

365 Overall, we hypothesize that two main processes are at work. First, we identify signatures
366 of turnover-driven speciation at shallow levels of the tree due to greater geographic isolation
367 among low-vagility species, and among deeper clades due to the survival of temperate lineages
368 in extratropical climates. We provide phylogenetic evidence supporting the notion that the
369 latitudinal diversity gradient is in fact a relatively young phenomenon in mammals, perhaps
370 originating or steepening during the Pliocene as the fossil record suggests (94). Second, we
371 hypothesize that persistence-driven speciation is occurring in diurnal lineages due to lower
372 extinction rates following access to new daytime niches and subsequent release from nocturnal
373 competitors. In this case, diurnality is an example of an adaptive innovation in mammals that is
374 presumably associated with greater ecological opportunity. Traversing from the first to second
375 macroevolutionary mode may be possible if otherwise ephemeral incipient species can enter
376 novel regimes of lower extinction risk, either via niche evolution or extrinsic opportunity (84,
377 98), to then differentially persist through time.

378 In summary, our study shows that coupling two ideas—that new species are formed
379 frequently but rarely persist (51), and extinction risk is related to species-level traits (27)—helps
380 to connect within-species dynamics of dispersal, gene flow, and niche evolution with

381 macroevolutionary rates. We logically reason that axes of low-to-high vagility and day-to-night
382 activity are affecting extinction rates in respectively opposite directions (i.e., high extinction and
383 turnover versus low extinction and turnover). However, the lack of direct extinction-rate
384 estimates is a clear shortcoming of this argument that can only be addressed by more fully
385 leveraging the mammal fossil record. Future tests that develop direct skeletal or remotely sensed
386 measurements of mammalian vagility (as opposed to the indirect index used here), along with
387 cranial correlates of diurnal vision (e.g., (97)), will be valuable for assessing whether the relative
388 frequency of turnover- and persistence-driven speciation has changed from fossil to modern
389 ecosystems. Efforts to connect evolutionary levels from individual organisms to speciose clades
390 appear the most promising for comprehending uneven species richness in the tree of life.
391
392 **METHODS**
393 **Mammalian phylogeny and species trait data.** We leveraged the recently constructed
394 species-level mammal trees of Upham et al. (35) to conduct all analyses. Briefly, these
395 phylogenies include 5,804 extant and 107 recently extinct species in credible sets of 10,000 trees.
396 They are built using a 'backbone-and-patch' framework that used two stages of Bayesian
397 inference to integrate age and topological uncertainty, and incorporate 1,813 DNA-lacking
398 species using probabilistic constraints (available at vertlife.org/phylosubsets). We compared
399 credible sets of trees built using node-dated backbones (17 fossil calibrations) and tip-dated
400 backbones (matrix of modern and Mesozoic mammals), as well as taxonomically completed
401 trees (5,911 species) versus trees of DNA-only species ($N = 4{,}098$) without topology constraints.
402 Our workflow for gathering trait data involved (i) unifying multiple trait taxonomies
403 (e.g., EltonTraits v1.0 (100), PanTHERIA (101)) to our phylogeny's master taxonomy; and (ii)
404 interpolating home range area and vagility to the species level using known allometric

relationships in mammals (Fig. S2). Vagility was calculated as the maximum natal dispersal distance per individual (km) and interpolated for each species following our updated version of Whitmee and Orme's (48) best-fit equation, which applies species means of body mass, home range, and geographic range (Fig. S3). Note that our vagility index does not account for locomotor abilities (e.g., flying or arboreality), but rather captures aspects of space use that scale allometrically across mammals.

Tip-level speciation rates. We calculated per-species estimates of expected pure-birth diversification rates for the instantaneous present moment (tips of the tree) using the inverse of the equal splits measure (77, 102). This metric has been called 'tip-level diversification rate' (tip DR) because it measures recent diversification processes among extant species (103). However, to avoid confusion with 'net diversification', for which tip DR is misleading when extinction is very high (relative extinction >0.8 (78)), we here refer to tip DR as a tip-level speciation rate metric. At the tip level, we show that tip DR is tightly associated with model-based estimators of speciation and net diversification rates in our trees (Fig. S1a). At the clade-level, we measure 'clade tip speciation mean' as the harmonic mean of tip DR among species, which is known to converge to the maximum likelihood estimator of pure-birth diversification rate in clades with >10 species (77, 102). We show that clade tip DR mean indeed best approximates pure-birth clade rates for time-sliced clades in our mammal trees (R^2: ~0.7 versus ~0.5 for birth-death speciation and net diversification rates; Fig. S1b).

Branch-specific and tree-wide rate shifts. We performed searches for macroevolutionary shifts using BAMM v2.5 (65), a reversible-jump algorithm for sampling birth-death rate regimes without a prior hypothesis. We evaluated the number and location of rate shifts on 10 trees from the node-dated sample of complete mammal trees. We summarized

428 across the most likely shifts per tree—called maximum shift credibility (MSC) sets (Fig. S7)—
429 using the ratio of the mean net diversification rate of all branches inside the shifted clade (clade
430 rate) and outside that clade (background rate) to calculate the rate shift magnitude and direction
431 for each MSC set (Table S1). For tree-wide rate shifts, we compared results from TreePar (41)
432 and CoMET (63) (see details in Fig. S5-S6).

433 **Comparisons with fossil genus diversification.** To assess the congruence of our
434 molecular phylogeny-based rate estimates with rates estimated from the fossil record, we
435 analyzed Mammalia fossil occurrence data from the Paleobiology Database (37). Grouping by
436 genus after excluding ichnotaxa and uncertain genera, we recovered 71,928 occurrences of 5300
437 genera, which we then binned in 10-Ma intervals (taxa spanning boundaries go in both bins) and
438 used shareholder quorum subsampling (SQS (104); quorum size: 0.5) to maximize the
439 uniformity of coverage. We then calculated corresponding origination and extinction rates per
440 stage using the per-capita rate method (105).

441 **Likelihood testing for models of diversification.** We analyzed the branching times of
442 27 named subclades (11 orders and 16 suborders) that contained ≥ 25 species. For each subclade,
443 we tested 10 models developed by Morlon et al. (70): two rate-constant (RC) models, constant
444 pure-birth and birth-death; and eight rate-variable (RV) models, with exponentially and linearly
445 time-varying rates. We fit models for 100 trees of the empirical subclades and their matching
446 RC-simulated trees (null models, simulated under the empirical extinction fractions of ~ε=0.65
447 over 100 trees using the "pbtree" function in phytools (106)). Subtracting AICc scores of the
448 best-fitting RC and RV models provided the ΔAIC_{RC-RV} test statistic (107) per tree and subclade
449 for comparison to the simulated null distribution (alpha=0.05; see Table S2).

Time-sliced clades and clade-level tests of species richness variation. To objectively define clades, we arbitrarily drew lines (referred to as "time slices") at 5-Ma intervals and took the resulting *tipward* (all the way to the extant tip) monophyletic clades as non-nested units of analysis. The *rootward* relationships of those clades (the "rootward backbone") was retained for each interval, giving the expected covariance structure among clades when performing phylogenetic generalized least squares (PGLS) analyses (see Fig. 3 for illustration). We used the "treeSlice" function in phytools to construct clade sets across Mammalia trees and the three sets of RC simulations, empirical (ε=0.65), low (ε=0.2), and high (ε=0.8), also comparing our results to analyses on traditional taxon-based clades (genera, families, and orders; Fig. S10-S12). All PGLS was performed excluding extinct species, using Pagel's "lambda" transformation in phylolm (optimized for large trees (108)), and repeating the analysis across 100 or 1000 trees. We also performed multivariate analyses including percent of DNA-sampled species per clade to test whether our results are unaffected by imputing DNA-missing species (Fig. S10).

Tip-level tests of speciation-rate correlates. To examine correlative structures underlying observed tip-rate variation, we performed tip-level PGLS analyses between species' ecological traits and tip DR values across 1000 trees, focusing on a 5675-species data set that excluded all extinct (n=107) and marine (n=129) species. We followed Freckleton et al. (82) in using trait ~ rate models in our tip-level PGLS analyses to avoid identical residuals in the dependent variable (i.e., sister species have identical tip DR values, which otherwise violates the assumed within-variable data independence in bivariate normal distributions). The trait ~ rate approach was previously applied using tip DR in univariate contexts (109) (see Fig. S13-S14 for sensitivity tests).

Clade-level tests of speciation-rate correlates. At the clade level, univariate PGLS was performed typically (rate ~ trait models), since clade tip DR mean gave independent values to sister clades. These analyses were conducted on 1000 trees by analogy with those previous, except that per-clade trait summaries were standardized predictors (mean centered, standard deviation scaled) using geometric means for vagility and arithmetic means otherwise. We also performed tests for trait-dependent speciation using rate-shifted clades identified in BAMM runs on 10 mammal trees (STRAPP (69) method), which corrects for phylogenetic pseudoreplication similar to PGLS except instead via the covariance structure among rate regimes (see Fig. S8).

Phylogenetic path analyses. We performed path analysis aiming to fully resolve correlational structures and thereby translate from the language of statistical association to causality. For phylogenetic path analyses, we used PGLS to test statements of conditional independence (60) across 27 pre-selected path models (Fig. S4). For each tree and clade set, we used "phylopath" (110) to analyze models and perform conditional model averaging. Time-sliced clades at 10-, 30-, and 50-Ma intervals were analyzed and compared to analogous results using taxon-based clades (Fig. S12; see *Supplementary Information* for further details).

Acknowledgments: We thank I. Quintero, M. Landis, D. Schluter, A. Mooers, A. Pyron, G. Thomas, D. Greenberg, S. Upham and E. Florsheim for conceptual discussions that improved this study; B. Patterson, K. Rowe, J. Brown, T. Colston, T. Peterson, D. Field, T. Stewart, J. Davies, and three anonymous reviewers for comments on earlier drafts; and M. Koo, A. Ranipeta, and J. Hart for database help. Artwork from phylopic.org and open source fonts.

Funding: The NSF VertLife Terrestrial grant to W.J. and J.E. (DEB 1441737 and 1441634) and NSF grant DBI-1262600 to W.J. supported this work. **Competing interests:** None.

References

1. P. V. A. Fine, R. H. Ree, Evidence for a Time-Integrated Species-Area Effect on the Latitudinal Gradient in Tree Diversity. *Am. Nat.* **168**, 796–804 (2006).
2. D. Jablonski, K. Roy, J. W. Valentine, Out of the Tropics: Evolutionary dynamics of the latitudinal diversity gradient. *Science* **314**, 102–106 (2006).
3. G. G. Mittelbach, *et al.*, Evolution and the latitudinal diversity gradient: speciation, extinction and biogeography. *Ecol. Lett.* **10**, 315–331 (2007).
4. W. Jetz, P. V. A. Fine, Global Gradients in Vertebrate Diversity Predicted by Historical Area-Productivity Dynamics and Contemporary Environment. *PLOS Biol.* **10**, e1001292 (2012).
5. R. Jansson, G. Rodríguez-Castañeda, L. E. Harding, What Can Multiple Phylogenies Say About the Latitudinal Diversity Gradient? A New Look at the Tropical Conservatism, Out of the Tropics, and Diversification Rate Hypotheses. *Evolution* **67**, 1741–1755 (2013).
6. J. C. Willis, *Age and Area* (Cambridge University Press, 1922).
7. A. O. Mooers, S. B. Heard, Inferring Evolutionary Process from Phylogenetic Tree Shape. *Q. Rev. Biol.* **72**, 31–54 (1997).
8. M. A. McPeek, J. M. Brown, Clade age and not diversification rate explains species richness among animal taxa. *Am. Nat.* **169** (2007).
9. J. J. Wiens, The causes of species richness patterns across space, time, and clades and the role of "ecological limits". *Q. Rev. Biol.* **86**, 75–96 (2011).
10. D. L. Rabosky, G. J. Slater, M. E. Alfaro, Clade age and species richness are decoupled across the eukaryotic tree of life. *PLoS Biol.* **10**, e1001381 (2012).
11. S. B. Hedges, J. Marin, M. Suleski, M. Paymer, S. Kumar, Tree of life reveals clock-like speciation and diversification. *Mol. Biol. Evol.*, msv037 (2015).
12. R. E. Ricklefs, Global diversification rates of passerine birds. *Proc. R. Soc. Lond. B-Biol. Sci.* **270**, 2285–2291 (2003).
13. M. G. B. Blum, O. François, Which Random Processes Describe the Tree of Life? A Large-Scale Study of Phylogenetic Tree Imbalance. *Syst. Biol.* **55**, 685–691 (2006).
14. A. B. Phillimore, T. D. Price, Density-dependent cladogenesis in birds. *PLoS Biol.* **6**, e71 (2008).
15. D. L. Rabosky, Ecological limits and diversification rate: alternative paradigms to explain the variation in species richness among clades and regions. *Ecol. Lett.* **12**, 735–743 (2009).
16. C. Venditti, A. Meade, M. Pagel, Phylogenies reveal new interpretation of speciation and the Red Queen. *Nature* **463**, 349–352 (2010).
17. T. J. Davies, A. P. Allen, L. Borda-de-Água, J. Regetz, C. J. Melián, Neutral Biodiversity Theory Can Explain the Imbalance of Phylogenetic Trees but Not the Tempo of Their Diversification. *Evolution* **65**, 1841–1850 (2011).
18. A. Purvis, S. A. Fritz, J. Rodríguez, P. H. Harvey, R. Grenyer, The shape of mammalian phylogeny: patterns, processes and scales. *Philos. Trans. R. Soc. Lond. B Biol. Sci.* **366**, 2462–2477 (2011).
19. D. S. Moen, H. Morlon, Why does diversification slow down? *Trends Ecol. Evol.* **29**, 190–197 (2014).
20. L. F. H. Diaz, L. J. Harmon, M. T. C. Sugawara, E. T. Miller, M. W. Pennell, Macroevolutionary diversification rates show time dependency. *Proc. Natl. Acad. Sci.*, 201818058 (2019).

21. A. Castro-Insua, C. Gómez-Rodríguez, J. J. Wiens, A. Baselga, Climatic niche divergence drives patterns of diversification and richness among mammal families. *Sci. Rep.* **8**, 8781 (2018).
22. S. A. Price, S. B. Hopkins, K. K. Smith, V. L. Roth, Tempo of trophic evolution and its impact on mammalian diversification. *Proc. Natl. Acad. Sci. USA* **109**, 7008–7012 (2012).
23. A. Machac, C. H. Graham, D. Storch, Ecological controls of mammalian diversification vary with phylogenetic scale. *Glob. Ecol. Biogeogr.* **27**, 32–46 (2018).
24. J. T. Weir, D. Schluter, The Latitudinal Gradient in Recent Speciation and Extinction Rates of Birds and Mammals. *Science* **315**, 1574–1576 (2007).
25. A. D. Cutter, J. C. Gray, Ephemeral ecological speciation and the latitudinal biodiversity gradient. *Evolution* **70**, 2171–2185 (2016).
26. A. Machac, C. H. Graham, Regional Diversity and Diversification in Mammals. *Am. Nat.* **189**, E1–E13 (2017).
27. D. Jablonski, Species Selection: Theory and Data. *Annu. Rev. Ecol. Evol. Syst.* **39**, 501–524 (2008).
28. J. Alroy, Small mammals have big tails in the tropics. *Glob. Ecol. Biogeogr.* **0** (2019).
29. D. M. Grossnickle, E. Newham, Therian mammals experience an ecomorphological radiation during the Late Cretaceous and selective extinction at the K–Pg boundary. *Proc R Soc B* **283**, 20160256 (2016).
30. D. J. Field, *et al.*, Early Evolution of Modern Birds Structured by Global Forest Collapse at the End-Cretaceous Mass Extinction. *Curr. Biol.* **28**, 1825-1831.e2 (2018).
31. D. M. Grossnickle, S. M. Smith, G. P. Wilson, Untangling the Multiple Ecological Radiations of Early Mammals. *Trends Ecol. Evol.* (2019) https:/doi.org/10.1016/j.tree.2019.05.008 (July 24, 2019).
32. J. S. Berv, D. J. Field, Genomic Signature of an Avian Lilliput Effect across the K-Pg Extinction. *Syst. Biol.* (2017) https:/doi.org/10.1093/sysbio/syx064 (December 7, 2017).
33. M. P. Gerkema, W. I. L. Davies, R. G. Foster, M. Menaker, R. A. Hut, The nocturnal bottleneck and the evolution of activity patterns in mammals. *Proc R Soc B* **280**, 20130508 (2013).
34. C. J. Burgin, J. P. Colella, P. L. Kahn, N. S. Upham, How many species of mammals are there? *J. Mammal.* **99**, 1–14 (2018).
35. N. S. Upham, J. A. Esselstyn, W. Jetz, Inferring the mammal tree: species-level sets of phylogenies for questions in ecology, evolution, and conservation. *PLOS Biol.* (2019).
36. T. W. Davies, M. A. Bell, A. Goswami, T. J. D. Halliday, Completeness of the eutherian mammal fossil record and implications for reconstructing mammal evolution through the Cretaceous/Paleogene mass extinction. *Paleobiology* (2017) https:/doi.org/10.1017/pab.2017.20 (October 7, 2018).
37. J. Alroy, *et al.*, Taxonomic occurrences of Mammalia recorded in Fossilworks, the Evolution of Terrestrial Ecosystems database, and the Paleobiology Database. Fossilworks. http://fossilworks.org. (2018).
38. C. V. Bennett, P. Upchurch, F. J. Goin, A. Goswami, Deep time diversity of metatherian mammals: implications for evolutionary history and fossil-record quality. *Paleobiology* **44**, 171–198 (2018).
39. R. W. Meredith, *et al.*, Impacts of the Cretaceous Terrestrial Revolution and KPg Extinction on Mammal Diversification. *Science* **334**, 521–524 (2011).

40. O. R. P. Bininda-Emonds, *et al.*, The delayed rise of present-day mammals. *Nature* **446**, 507–512 (2007).
41. T. Stadler, Mammalian phylogeny reveals recent diversification rate shifts. *Proc. Natl. Acad. Sci.* **108**, 6187–6192 (2011).
42. J. Rolland, F. L. Condamine, F. Jiguet, H. Morlon, Faster Speciation and Reduced Extinction in the Tropics Contribute to the Mammalian Latitudinal Diversity Gradient. *PLOS Biol.* **12**, e1001775 (2014).
43. T. S. Kuhn, A. Ø. Mooers, G. H. Thomas, A simple polytomy resolver for dated phylogenies. *Methods Ecol. Evol.* **2**, 427–436 (2011).
44. S. Faurby, J.-C. Svenning, A species-level phylogeny of all extant and late Quaternary extinct mammals using a novel heuristic-hierarchical Bayesian approach. *Mol. Phylogenet. Evol.* **84**, 14–26 (2015).
45. J. D. Archibald, D. H. Deutschman, Quantitative Analysis of the Timing of the Origin and Diversification of Extant Placental Orders. *J. Mamm. Evol.* **8**, 107–124 (2001).
46. E. Mayr, *Animal species and evolution* (Belknap, 1963).
47. Y. Kisel, T. G. Barraclough, Speciation Has a Spatial Scale That Depends on Levels of Gene Flow. *Am. Nat.* **175**, 316–334 (2010).
48. S. Whitmee, C. D. L. Orme, Predicting dispersal distance in mammals: a trait-based approach. *J. Anim. Ecol.* **82**, 211–221 (2013).
49. Belliure, Sorci, Møller, Clobert, Dispersal distances predict subspecies richness in birds. *J. Evol. Biol.* **13**, 480–487 (2000).
50. S. Claramunt, E. P. Derryberry, J. V. Remsen, R. T. Brumfield, High dispersal ability inhibits speciation in a continental radiation of passerine birds. *Proc. R. Soc. Lond. B Biol. Sci.* **279**, 1567–1574 (2012).
51. E. B. Rosenblum, *et al.*, Goldilocks Meets Santa Rosalia: An Ephemeral Speciation Model Explains Patterns of Diversification Across Time Scales. *Evol. Biol.* **39**, 255–261 (2012).
52. D. Schluter, M. W. Pennell, Speciation gradients and the distribution of biodiversity. *Nature* **546**, 48–55 (2017).
53. Soria-Carrasco Víctor, Castresana Jose, Diversification rates and the latitudinal gradient of diversity in mammals. *Proc. R. Soc. B Biol. Sci.* **279**, 4148–4155 (2012).
54. C. A. Botero, R. Dor, C. M. McCain, R. J. Safran, Environmental harshness is positively correlated with intraspecific divergence in mammals and birds. *Mol. Ecol.* **23**, 259–268 (2014).
55. R. Maor, T. Dayan, H. Ferguson-Gow, K. E. Jones, Temporal niche expansion in mammals from a nocturnal ancestor after dinosaur extinction. *Nat. Ecol. Evol.* **1**, 1889 (2017).
56. S. R. Anderson, J. J. Wiens, Out of the dark: 350 million years of conservatism and evolution in diel activity patterns in vertebrates: EVOLUTION OF DAY-NIGHT ACTIVITY PATTERNS. *Evolution* **71**, 1944–1959 (2017).
57. K. Magnuson-Ford, S. P. Otto, Linking the Investigations of Character Evolution and Species Diversification. *Am. Nat.* **180**, 225–245 (2012).
58. L. Santini, D. Rojas, G. Donati, Evolving through day and night: origin and diversification of activity pattern in modern primates. *Behav. Ecol.* **26**, 789–796 (2015).
59. J. M. Beaulieu, B. C. O'Meara, Can we build it? Yes we can, but should we use it? Assessing the quality and value of a very large phylogeny of campanulid angiosperms. *Am. J. Bot.* **105**, 417–432 (2018).

60. A. von Hardenberg, A. Gonzalez-Voyer, Disentangling Evolutionary Cause-Effect Relationships with Phylogenetic Confirmatory Path Analysis. *Evolution* **67**, 378–387 (2013).
61. M. S. Springer, N. M. Foley, P. L. Brady, J. Gatesy, W. J. Murphy, Evolutionary Models for the Diversification of Placental Mammals Across the KPg Boundary. *Front. Genet.* **10** (2019).
62. M. dos Reis, *et al.*, Phylogenomic datasets provide both precision and accuracy in estimating the timescale of placental mammal phylogeny. *Proc. R. Soc. Lond. B Biol. Sci.* **279**, 3491–3500 (2012).
63. M. R. May, S. Höhna, B. R. Moore, A Bayesian approach for detecting the impact of mass-extinction events on molecular phylogenies when rates of lineage diversification may vary. *Methods Ecol. Evol.* **7**, 947–959 (2016).
64. M. M. Pires, B. D. Rankin, D. Silvestro, T. B. Quental, Diversification dynamics of mammalian clades during the K–Pg mass extinction. *Biol. Lett.* **14**, 20180458 (2018).
65. D. L. Rabosky, Automatic detection of key innovations, rate shifts, and diversity-dependence on phylogenetic trees. *PLoS ONE* **9**, e89543 (2014).
66. B. R. Moore, K. M. A. Chan, M. J. Donoghue, "Detecting Diversification Rate Variation in Supertrees" in *Phylogenetic Supertrees*, Computational Biology., O. R. P. Bininda-Emonds, Ed. (Springer Netherlands, 2004), pp. 487–533.
67. S. Nee, E. C. Holmes, R. M. May, P. H. Harvey, Extinction rates can be estimated from molecular phylogenies. *Philos. Trans. R. Soc. Lond. B-Biol. Sci.* **344**, 77–82 (1994).
68. J. J. Schenk, K. C. Rowe, S. J. Steppan, Ecological opportunity and incumbency in the diversification of repeated continental colonizations by muroid rodents. *Syst. Biol.* **62**, 837–864 (2013).
69. D. L. Rabosky, H. Huang, A Robust Semi-Parametric Test for Detecting Trait-Dependent Diversification. *Syst. Biol.* **65**, 181–193 (2016).
70. H. Morlon, T. L. Parsons, J. B. Plotkin, Reconciling molecular phylogenies with the fossil record. *Proc. Natl. Acad. Sci.* **108**, 16327–16332 (2011).
71. S. Louca, M. W. Pennell, Phylogenies of extant species are consistent with an infinite array of diversification histories. *bioRxiv*, 719435 (2019).
72. J. L. Cantalapiedra, J. L. Prado, M. H. Fernández, M. T. Alberdi, Decoupled ecomorphological evolution and diversification in Neogene-Quaternary horses. *Science* **355**, 627–630 (2017).
73. G. Burin, L. R. V. Alencar, J. Chang, M. E. Alfaro, T. B. Quental, How Well Can We Estimate Diversity Dynamics for Clades in Diversity Decline? *Syst. Biol.* **68**, 47–62 (2019).
74. N. D. Pyenson, The Ecological Rise of Whales Chronicled by the Fossil Record. *Curr. Biol.* **27**, R558–R564 (2017).
75. J. J. Shi, D. L. Rabosky, Speciation dynamics during the global radiation of extant bats. *Evolution* **69**, 1528–1545 (2015).
76. L. I. Amador, R. L. M. Arévalo, F. C. Almeida, S. A. Catalano, N. P. Giannini, Bat Systematics in the Light of Unconstrained Analyses of a Comprehensive Molecular Supermatrix. *J. Mamm. Evol.* **25**, 37–70 (2018).
77. W. Jetz, G. H. Thomas, J. B. Joy, K. Hartmann, A. O. Mooers, The global diversity of birds in space and time. *Nature* **491**, 444–448 (2012).
78. P. O. Title, D. L. Rabosky, Tip rates, phylogenies and diversification: What are we estimating, and how good are the estimates? *Methods Ecol. Evol.* **10**, 821–834 (2019).

79. U. Kodandaramaiah, G. Murali, What affects power to estimate speciation rate shifts? *PeerJ* **6**, e5495 (2018).
80. T. D. Price, The roles of time and ecology in the continental radiation of the Old World leaf warblers (*Phylloscopus* and *Seicercus*). *Philos. Trans. R. Soc. Lond. B Biol. Sci.* **365**, 1749–1762 (2010).
81. S. Wright, The "Age and Area" Concept Extended. *Ecology* **22**, 345–347 (1941).
82. R. P. Freckleton, A. B. Phillimore, M. Pagel, Relating Traits to Diversification: A Simple Test. *Am. Nat.* **172**, 102–115 (2008).
83. D. Jablonski, Larval ecology and macroevolution in marine invertebrates. *Bull. Mar. Sci.* **39**, 565–587 (1986).
84. J. B. Yoder, *et al.*, Ecological opportunity and the origin of adaptive radiations. *J. Evol. Biol.* **23**, 1581–1596 (2010).
85. A. D. Davidson, M. J. Hamilton, A. G. Boyer, J. H. Brown, G. Ceballos, Multiple ecological pathways to extinction in mammals. *Proc. Natl. Acad. Sci.* **106**, 10702–10705 (2009).
86. S. Faurby, J.-C. Svenning, Resurrection of the Island Rule: Human-Driven Extinctions Have Obscured a Basic Evolutionary Pattern. *Am. Nat.* **187**, 812–820 (2016).
87. U. M. L. Norberg, J. Rayner, Ecological morphology and flight in bats (Mammalia; Chiroptera): wing adaptations, flight performance, foraging strategy and echolocation. *Philos. Trans. R. Soc. Lond. B Biol. Sci.* **316**, 335–427 (1987).
88. D. L. Rabosky, P. O. Title, H. Huang, Minimal effects of latitude on present-day speciation rates in New World birds. *Proc R Soc B* **282**, 20142889 (2015).
89. J. D. Kennedy, *et al.*, Into and out of the tropics: the generation of the latitudinal gradient among New World passerine birds. *J. Biogeogr.* **41**, 1746–1757 (2014).
90. B. Nabholz, S. Glémin, N. Galtier, The erratic mitochondrial clock: variations of mutation rate, not population size, affect mtDNA diversity across birds and mammals. *BMC Evol. Biol.* **9**, 54 (2009).
91. P. R. Martin, J. J. Tewksbury, Latitudinal Variation in Subspecific Diversification of Birds. *Evolution* **62**, 2775–2788 (2008).
92. M. Mudelsee, M. E. Raymo, Slow dynamics of the Northern Hemisphere glaciation. *Paleoceanography* **20** (2005).
93. G. Hewitt, The genetic legacy of the Quaternary ice ages. *Nature* **405**, 907–913 (2000).
94. J. D. Marcot, D. L. Fox, S. R. Niebuhr, Late Cenozoic onset of the latitudinal diversity gradient of North American mammals. *Proc. Natl. Acad. Sci.* **113**, 7189–7194 (2016).
95. D. Jablonski, S. Huang, K. Roy, J. W. Valentine, Shaping the Latitudinal Diversity Gradient: New Perspectives from a Synthesis of Paleobiology and Biogeography. *Am. Nat.* **189**, 1–12 (2016).
96. J. H. Arbour, S. E. Santana, A major shift in diversification rate helps explain macroevolutionary patterns in primate species diversity. *Evolution* **71**, 1600–1613 (2017).
97. K. D. Angielczyk, L. Schmitz, Nocturnality in synapsids predates the origin of mammals by over 100 million years. *Proc. R. Soc. B Biol. Sci.* **281**, 20141642 (2014).
98. G. G. Simpson, *The major features of evolution* (Columbia Univ Press, 1953).
99. M. L. Zelditch, J. Li, L. A. P. Tran, D. L. Swiderski, Relationships of diversity, disparity, and their evolutionary rates in squirrels (Sciuridae). *Evolution* **69**, 1284–1300 (2015).
100. H. Wilman, *et al.*, EltonTraits 1.0: Species-level foraging attributes of the world's birds and mammals. *Ecology* **95**, 2027–2027 (2014).

101. K. E. Jones, *et al.*, PanTHERIA: a species-level database of life history, ecology, and geography of extant and recently extinct mammals. *Ecology* **90**, 2648–2648 (2009).
102. M. Steel, A. Mooers, The expected length of pendant and interior edges of a Yule tree. *Appl. Math. Lett.* **23**, 1315–1319 (2010).
103. I. Quintero, W. Jetz, Global elevational diversity and diversification of birds. *Nature* (2018) (February 21, 2018).
104. J. Alroy, Accurate and precise estimates of origination and extinction rates. *Paleobiology* **40**, 374–397 (2014).
105. M. Foote, Origination and extinction components of taxonomic diversity: general problems. *Paleobiology* **26**, 74–102 (2000).
106. L. J. Revell, phytools: an R package for phylogenetic comparative biology (and other things). *Methods Ecol. Evol.* **3**, 217–223 (2012).
107. D. L. Rabosky, Likelihood methods for detecting temporal shifts in diversification rates. *Evolution* **60**, 1152–1164 (2006).
108. L. S. T. Ho, C. Ané, A Linear-Time Algorithm for Gaussian and Non-Gaussian Trait Evolution Models. *Syst. Biol.* **63**, 397–408 (2014).
109. M. G. Harvey, *et al.*, Positive association between population genetic differentiation and speciation rates in New World birds. *Proc. Natl. Acad. Sci.* **114**, 6328–6333 (2017).
110. W. van der Bijl, phylopath: Easy phylogenetic path analysis in R. *PeerJ* **6**, e4718 (2018).

741 **Figure legends**

742 **Fig. 1. Species-level relationships, rates, and traits for 5,911 species of mammals globally.**
743 (**a**) The maximum clade credibility topology of 10,000 node-dated trees, with numbered clade
744 labels corresponding to orders and subclades listed in the plot periphery: Eulipoty., Eulipotyphla;
745 Carn., Carnivora; Artio., Artiodactyla. Scale in millions of years, Ma. Branches are colored with
746 tip-level speciation rates (tip DR metric) and marked with 24 inferred shifts in branch-specific
747 net diversification rates (nodes A-X; shifts with multiple circles occurred on either branch, not
748 both, over a sampling of 10 trees from the credible set). Tip-level rates are reconstructed to
749 interior branches using Brownian motion. (**b**) Per-species ecological traits: allometric index of
750 vagility (dispersal ability), diurnality (predominant daytime activity), and north-south latitudinal
751 extent (see *Methods* for details). Silhouettes are from phylopic.org and open source fonts.

752 **Fig. 2. Diversification rate variation among mammal clades.** Lineage-through-time plots and
753 estimated crown ages for (**a**) all superordinal divergences (y-axis does not apply to error bars),
754 and (**b**) placental orders with crown age estimates overlapping the Cretaceous-Paleogene
755 extinction event (K-Pg, dashed gray line; means and 95% CIs; filled circle if statistically
756 different). (**c**) Rate-through-time plots for speciation, extinction, and net diversification
757 (summarized from Fig. 1 rate shift analyses; medians from 10 trees, 95% CIs in light gray). (**d**)
758 Fossil genus diversity through time for all Mammalia, including subsampled genus richness
759 (quorum 0.5) and per-capita rates of genus origination and extinction. (**e**) Extant rates and
760 lineage-specific rate shifts for the five most speciose mammal orders (same symbols as in **c**). (**f**)
761 Rate variation within subclades of these five orders as numbered from Fig. 1; left: difference in
762 AIC between best-fit models of diversification for trees simulated under rate-constant birth-death
763 (gray) versus observed mammal trees (color; filled circle and * if ΔAIC on 100 trees is

764 statistically different); and, right: tip-level speciation rate (tip DR metric) distributions of the
765 same simulated and observed subclades (gray versus color, one tree), comparing variation in
766 clade tip rate mean and skew across 100 trees. The last 2 Ma are removed from parts **c-e** to focus
767 on pre-recent rate dynamics.

768 **Fig. 3. Explanation of time-sliced clade delimitation and summarization for testing**
769 **hypotheses.** (**a and b**) An example subclade (rodent family Heteromyidae; 64 species) is divided
770 into time-sliced clades in the same way as the Fig. 4 and 5 analyses of all Mammalia. Branch
771 colors in the subclade phylogeny correspond to tip-level speciation rates (tip DR metric)
772 calculated on the full tree, and red symbols are sized according to estimates of species vagility.
773 An example time slice for 5-Ma tipward clades is shown with summaries of tip rate mean and
774 vagility (harmonic and geometric means, respectively), which are then compared to clade crown
775 age and species richness. (**c**) Example of how time-sliced clades are analyzed across Mammalia,
776 here showing 35-Ma clades used to test for relationships among log clade richness and three
777 predictors in a multivariate PGLS analysis (phylogenetic generalized least squares). This PGLS
778 analysis was then repeated across a sample of 100 or 1000 trees from the credible set, and across
779 time-sliced clade delimitations every 5 Ma from 5-70 Ma, in each case comparing observed
780 mammal clades to clades from simulated rate-constant trees of the same crown age and species
781 richness (colors indicate different extinction fractions used). (**d**) Results for observed mammal
782 clades (grey) defined at time-slices every 5 Ma for log clade richness and its variance, as
783 compared to simulated trees (colors).

784 **Fig. 4. Age and rate components of species richness variation across time-sliced clades.** The
785 log species richness of time-sliced clades every 5 Ma, with clades defined tipward by dotted lines
786 as illustrated in Fig. 3, across a sample of 100 phylogenies is best predicted jointly by **(a)** clade

crown age, (**b**) clade tip-level speciation rate mean (harmonic mean of species' tip DR in clade), and (**c**) clade tip-level speciation rate skew (asymmetry of species' tip DR in clade; multivariate PGLS [phylogenetic generalized least squares] on standardized data with 95% confidence intervals [CIs] on parameter estimates). Clade tip rate mean explains most of the variation in species richness across time-sliced clades, given its consistently larger unique effects in observed clades (grey symbols and black line) than either clade crown age or tip rate skew. By comparing these observed effects on clade richness to simulated rate-constant effects (colored symbols and dashed lines; different extinction fractions, ε), we find that tip rate mean has significantly stronger effects on richness than expected from simulated birth-death trees containing only stochastic rate variation. Clade tip rate skew also explains significantly more variation in clade richness than expected at deeper time slices, while crown age matches the simulated predictions. Other predictors were also assessed, as were taxon-delimited clades (Fig. S10). Solid black lines connect the observed best-fitting models across time slices and trees.

Fig. 5. Connecting clade ages, rates, richness, and traits in the mammal tree of life. (**a**, top panel) Distribution of tip-level speciation rates (tip DR metric, harmonic mean of 10,000 trees) relative to per-species estimates of vagility (allometric index of maximum natal dispersal distance), diurnality (0=nocturnal or cathemeral, 1=diurnal), and absolute value of latitude (centroid of expert maps) across 5,675 species, excluding extinct and marine species. Loess smoothing lines visualize general trends without considering phylogeny (blue, span=0.33). (**a**, bottom panel) Species-level effects considering phylogeny between tip speciation rates and ecological traits, as subset across trophic levels of herbivores, omnivores, and carnivores (N = 1637, 1852, and 1565, respectively; univariate PGLS [phylogenetic generalized least squares] conducted on standardized predictors across 1000 trees, showing 95% confidence intervals of

slopes; colored if effects are significant, red for negative, blue for positive, else gray). (**b**) Phylogenetic path analysis conducted across time-sliced clades at 10-, 30-, and 50-Ma intervals, delimited as illustrated in Fig. 3 (nested multivariate PGLS on standardized data). This causal framework connects clade-level summaries of species' vagility (geometric mean), diurnality (arithmetic mean), and latitude (arithmetic mean of centroid absolute values) to corresponding clade rates, and those rates to clade species richness. Path thickness, color, and directionality denote median coefficients of model-averaged analyses across 1000 trees (see legend: positive paths in shades of blue, negative in shades of red; time-sliced clades of 10-, 30-, and 50-Ma proceed from left to right as labeled). The bottom panels provide per-estimate uncertainty across time slices (slope ± SE), with non-zero estimates totaled in the right margin. Paths present in >500 trees are bolded and displayed in the upper path model diagram whereas other paths are dashed lines.

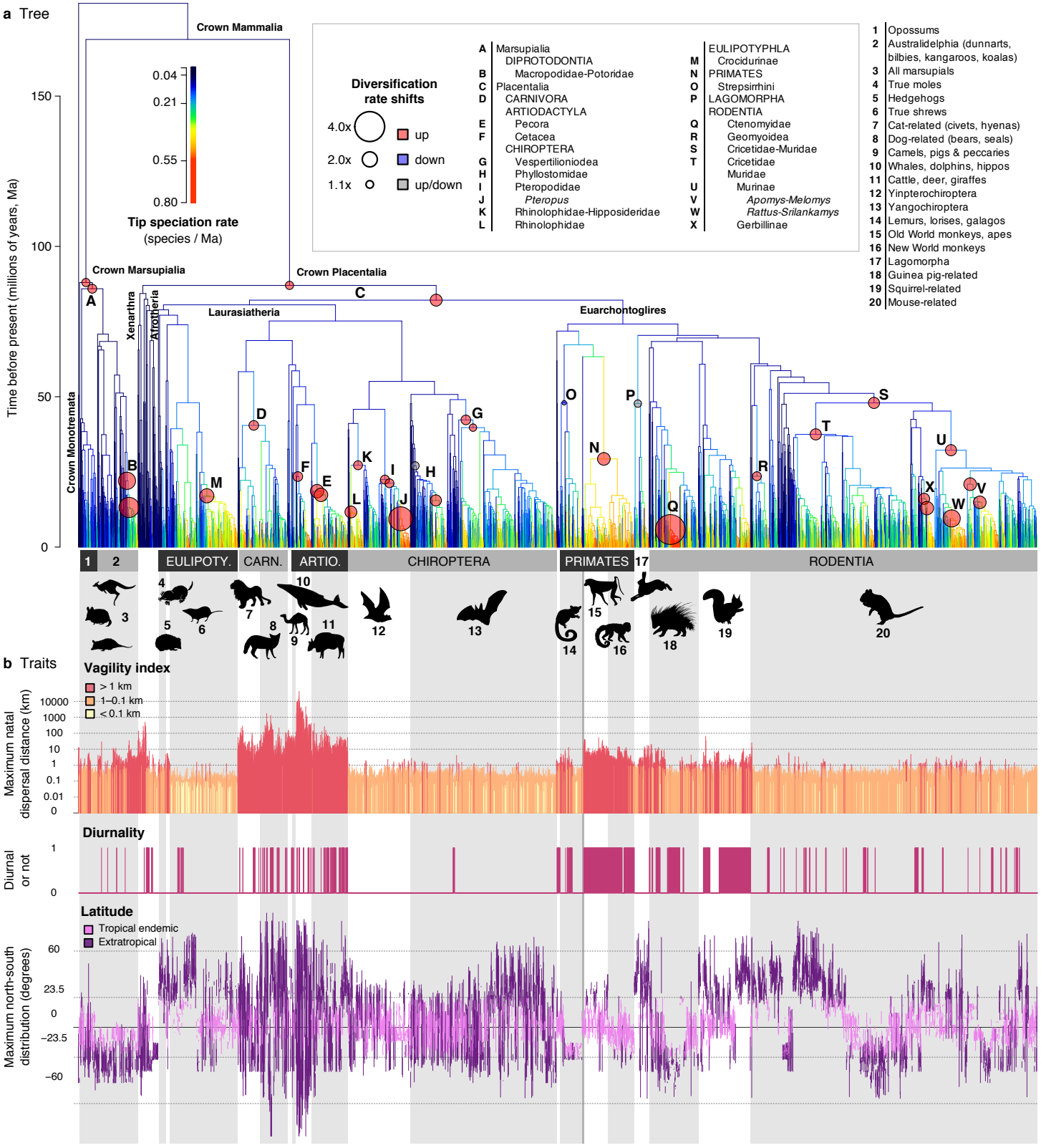

Fig. 1. Species-level relationships, rates, and traits for 5,911 species of mammals globally. (a) The maximum clade credibility topology of 10,000 node-dated trees, with numbered clade labels corresponding to orders and subclades listed in the plot periphery: Eulipoty., Eulipotyphla; Carn., Carnivora; Artio., Artiodactyla. Scale in millions of years, Ma. Branches are colored with tip-level speciation rates (tip DR metric) and marked with 24 inferred shifts in branch-specific net diversification rates (nodes A-X; shifts with multiple circles occurred on either branch, not both, over a sampling of 10 trees from the credible set). Tip-level rates are reconstructed to interior branches using Brownian motion. (**b**) Per-species ecological traits: allometric index of vagility (dispersal ability), diurnality (predominant daytime activity), and north-south latitudinal extent (see *Methods* for details). Silhouettes are from phylopic.org and open source fonts.

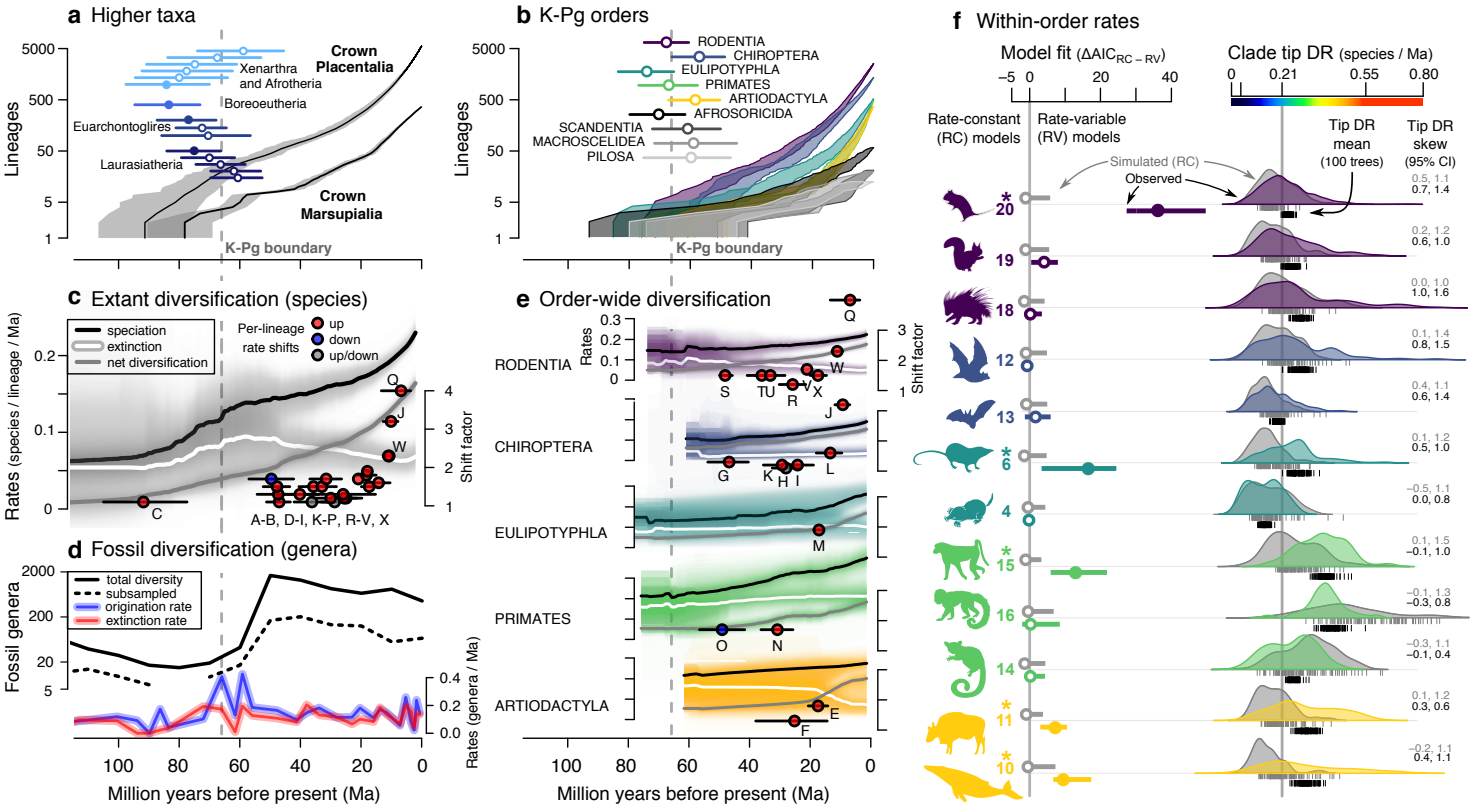

Fig. 2. Diversification rate variation among mammal clades. Lineage-through-time plots and estimated crown ages for (**a**) all superordinal divergences (y-axis does not apply to error bars), and (**b**) placental orders with crown age estimates overlapping the Cretaceous-Paleogene extinction event (K-Pg, dashed grey line; means and 95% CIs; filled circle if statistically different). (**c**) Extant rates of speciation, extinction, and net diversification through time on the full Mammalia phylogeny relative to lineage-specific shifts in net diversification (median rates from 10 trees, 95% CIs in light grey). (**d**) Fossil genus diversity through time for all Mammalia, including subsampled genus richness (quorum 0.5) and per-capita rates of genus origination and extinction. (**e**) Extant rates and lineage-specific rate shifts for the five most speciose mammal orders (same symbols as in **c**). (**f**) Rate variation within subclades of these five orders (numbers correspond to Fig. 1); left: quantified as difference in AIC between best-fit models of diversification ($\Delta AIC_{RC\text{-}RV}$ median and 95% CIs on 100 trees) for trees simulated under rate-constant birth-death (RC, grey) versus observed mammal trees (colour; * and filled circle if statistically different); and, right: example tip DR distributions of the same simulated and observed subclades (grey versus colour, one tree), comparing variation in tip DR mean and skew relative to the median for all Mammalia (grey line, 100 trees). The last 2 Ma are removed from parts **c-e** to focus on pre-recent rate dynamics.

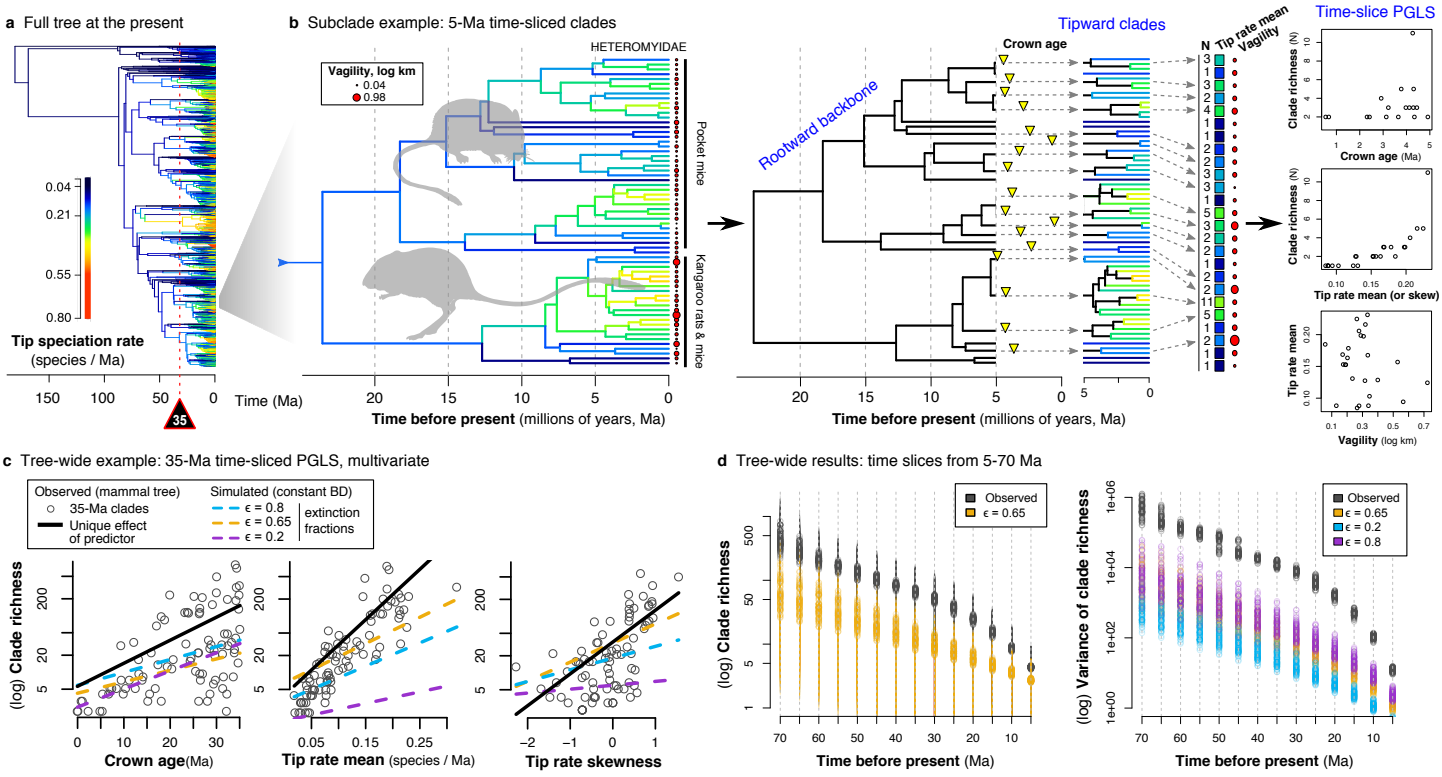

Fig. 3. Explanation of time-sliced clade delimitation and summarization for testing hypotheses. (**a and b**) An example subclade (rodent family Heteromyidae; 64 species) is divided into time-sliced clades in the same way as the Fig. 4 and 5 analyses of all Mammalia. Branch colors in the subclade phylogeny correspond to tip-level speciation rates (tip DR metric) calculated on the full tree, and red symbols are sized according to estimates of species vagility. An example time slice for 5-Ma tipward clades is shown with summaries of tip rate mean and vagility (harmonic and geometric means, respectively), which are then compared to clade crown age and species richness. (**c**) Example of how time-sliced clades are analyzed across Mammalia, here showing 35-Ma clades used to test for relationships among log clade richness and three predictors in a multivariate PGLS analysis (phylogenetic generalized least squares). This PGLS analysis was then repeated across a sample of 100 or 1000 trees from the credible set, and across time-sliced clade delimitations every 5 Ma from 5-70 Ma, in each case comparing observed mammal clades to clades from simulated rate-constant trees of the same crown age and species richness (colors indicate different extinction fractions used). (**d**) Results for observed mammal clades (grey) defined at time-slices every 5 Ma for log clade richness and its variance, as compared to simulated trees (colors).

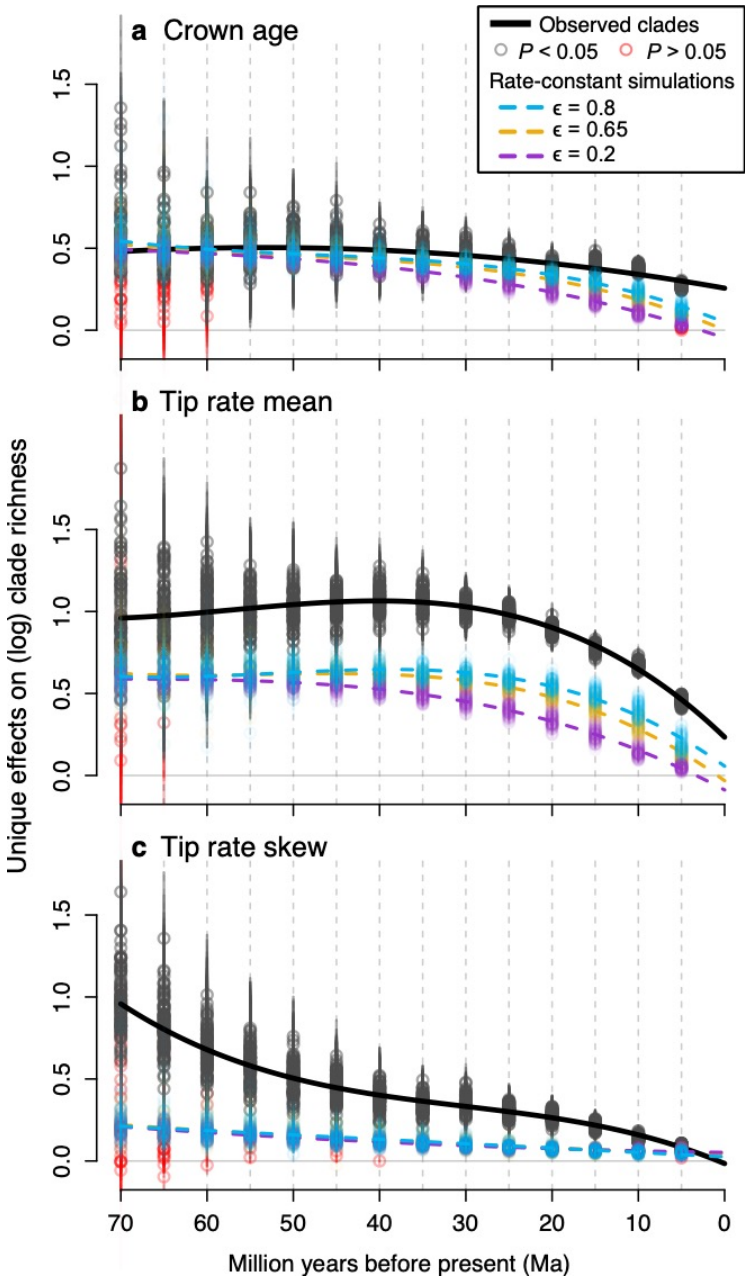

Fig. 4. Age and rate components of species richness variation across time-sliced clades. The log species richness of time-sliced clades every 5 Ma, with clades defined tipward by dotted lines as illustrated in Fig. 3, across a sample of 100 phylogenies is best predicted jointly by **(a)** clade crown age, (**b**) clade tip-level speciation rate mean (harmonic mean of species' tip DR in clade), and (**c**) clade tip-level speciation rate skew (asymmetry of species' tip DR in clade; multivariate PGLS [phylogenetic generalized least squares] on standardized data with 95% confidence intervals [CIs] on parameter estimates). Clade tip rate mean explains most of the variation in species richness across time-sliced clades, given its consistently larger unique effects in observed clades (grey symbols and black line) than either clade crown age or tip rate skew. By comparing these observed effects on clade richness to simulated rate-constant effects (colored symbols and dashed lines; different extinction fractions, ε), we find that tip rate mean has significantly stronger effects on richness than expected from simulated birth-death trees containing only stochastic rate variation. Clade tip rate skew also explains significantly more variation in clade richness than expected at deeper time slices, while crown age matches the simulated predictions. Other predictors were also assessed, as were taxon-delimited clades (Fig. S10). Solid black lines connect the observed best-fitting models across time slices and trees.

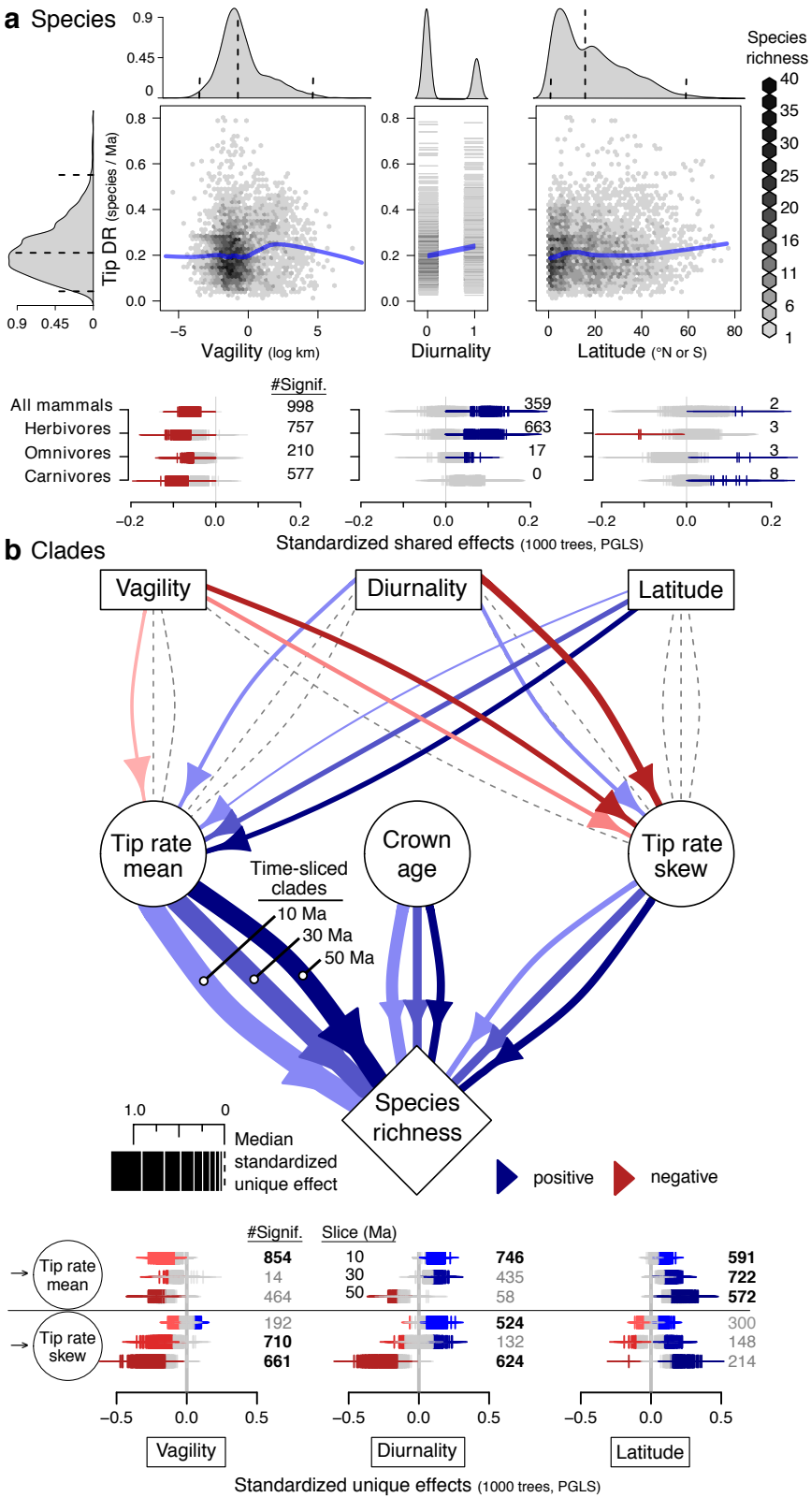

Fig. 5. Connecting clade ages, rates, richness, and traits in the mammal tree of life. (**a**, top panel) Distribution of tip-level speciation rates (tip DR metric, harmonic mean of 10,000 trees) relative to per-species estimates of vagility (allometric index of maximum natal dispersal distance), diurnality (0=nocturnal or cathemeral, 1=diurnal), and absolute value of latitude (centroid of expert maps) across 5,675 species, excluding extinct and marine species. Loess smoothing lines visualize general trends without considering phylogeny (blue, span=0.33). (**a**, bottom panel) Species-level effects considering phylogeny between tip speciation rates and ecological traits, as subset across trophic levels of herbivores, omnivores, and carnivores (N = 1637, 1852, and 1565, respectively; univariate PGLS [phylogenetic generalized least squares] conducted on standardized predictors across 1000 trees, showing 95% confidence intervals of slopes; colored if effects are significant, red for negative, blue for positive, else gray). (**b**) Phylogenetic path analysis conducted across time-sliced clades at 10-, 30-, and 50-Ma intervals, delimited as illustrated in Fig. 3 (nested multivariate PGLS on standardized data). This causal framework connects clade-level summaries of species' vagility (geometric mean), diurnality (arithmetic mean), and latitude (arithmetic mean of centroid absolute values) to corresponding clade rates, and those rates to clade species richness. Path thickness, color, and directionality denote median coefficients of model-averaged analyses across 1000 trees (see legend: positive paths in shades of blue, negative in shades of red; time-sliced clades of 10-, 30-, and 50-Ma proceed from left to right as labeled). The bottom panels provide per-estimate uncertainty across time slices (slope ± SE), with non-zero estimates totaled in the right margin. Paths present in >500 trees are bolded and displayed in the upper path model diagram whereas other paths are dashed lines.